The Journal of Veterinary Medical Science

FULL PAPER
Internal Medicine

Effect of acute volume loading on left atrial strain values derived from two-dimensional speckle tracking echocardiography in dogs

Angkhana DERMLIM[1)#], Tatsuyuki OSUGA[1)#], Kensuke NAKAMURA[2)*], Tomoya MORITA[1)], Khoirun NISA[1)], Kazuyoshi SASAOKA[1)], Rommaneeya LEELA-ARPORN[1)], Noriyuki NAGATA[1)], Masahiro TAMURA[1)], Noboru SASAKI[1)], Hiroshi OHTA[1)] and Mitsuyoshi TAKIGUCHI[1)]

[1)]Laboratory of Veterinary Internal Medicine, Graduate School of Veterinary Medicine, Hokkaido University, Hokkaido 006-0818, Japan
[2)]Laboratory of Internal Medicine, Organization for Promotion of Tenure Track, University of Miyazaki, Miyazaki 889-2192, Japan

ABSTRACT. The purpose of this study was to evaluate the cardiac acute volume loading effect on left atrial (LA) strain and strain rate (SR) parameters derived from two-dimensional speckle tracking echocardiography (2D-STE) in healthy dogs. Six healthy beagles were anesthetized and subjected to increase cardiac preload by intravenous infusion with lactated Ringer solution at 150 ml/kg/hr for 90 min. A Swan-Ganz catheter was placed to directly measure the mean pulmonary capillary wedge pressure (PCWP). Echocardiography was performed before (baseline) and at 15, 30, 45, 60, 75, and 90 min after acute volume loading began. Apical 4-chamber images focused on the LA were digitally recorded for later strain and SR analysis via 2D-STE. Acute volume loading significantly increased from baseline during LA strain and SR as assessed by the speckle tracking–based technique during reservoir and conduit function at 15 to 90 min after volume load began, and strain indices representing booster pump function were enhanced at 45 to 90 min. In addition, acute volume loading resulted in a significantly greater PCWP after fluid infusion. On multiple regression analysis, quadratic regression analysis was a better fit for the relationship between PCWP and all LA functional indices. Our findings indicated that LA function analyzed by strain and SR was enhanced during cardiac acute volume loading in healthy dogs. The change in strain and SR during acute volume loading should be interpreted with caution during the diagnosis of heart diseases related to volume overload.

KEY WORDS: canine, deformation analysis, echocardiography, left atrial function, volume overload

J. Vet. Med. Sci.
81(7): 949–957, 2019
doi: 10.1292/jvms.19-0012

Received: 10 January 2019
Accepted: 24 April 2019
Advanced Epub:
15 May 2019

The left atrium (LA) serves three major roles in maintaining left ventricular (LV) filling and overall cardiovascular performance: a reservoir that stores pulmonary venous return during LV contraction [11], a conduit that continues to passively transfer pulmonary venous flow during LV diastole, and a booster pump function that actively augments LV filling during atrial systole [31]. LA function helps to preserve cardiac output and maintain an effective LV stroke volume [21, 22, 29]. In patients with LV dysfunction, the importance of the atrial contribution to ventricular filling is emphasized by the development of clinical signs and symptoms of heart failure when LA contraction is impaired [24, 30].

In humans, the method that accurately determines the values of LA area and volume are two-dimensional (2D) echocardiography, multislice computed tomography, cardiac magnetic resonance imaging, and real time three-dimensional echocardiography [12, 32]. In veterinary patients, the phasic size of the LA (area and volume) [1, 2, 6, 13, 14, 19, 26, 28, 34] and the percentage fractional area change using 2D echocardiography have been an area of focus because of their utility in measuring LA function [14, 19, 26, 28].

A novel echocardiographic technique on the basis of the 2D speckle tracking method enabled automatic analysis of the time-LA area or volume curve representing LA phasic function in humans [20, 23] and dogs [14, 28]. The LA fractional area change during booster pump function (LA-FAC_{act}) obtained via two-dimensional speckle tracking echocardiography (2D-STE) was lower in dogs with progressively more severe myxomatous mitral valvular heart disease [1, 26].

*Correspondence to: Nakamura, K.: kenvet@cc.miyazaki-u.ac.jp
#These authors contributed equally to this work.

Moreover, strain imaging using 2D-STE is currently being developed for quantification of LA myocardial deformation by tracking the LA wall from frame to frame throughout the cardiac cycle and focuses on calculating the deformation parameter (strain) and the rate of deformation change (strain rate [SR]) automatically [1, 5, 25]. Notably, LA booster pump dysfunction indicated by strain imaging using 2D-STE was shown to be the best predictor of heart failure complications in dogs and had a higher predictive power for evaluating congestive heart failure over the LA-FAC_{act} [25].

Volume load dependency of echocardiographic indices is of clinical concern when using the indices in heart diseases associated with volume overload: LA dysfunction can be masked by the enhancing effect of the volume loading on LA function indices [31]. In a previous experimental study using healthy beagles, we have shown that the volumetric LA function indices (i.e., LA fractional area changes) determined with 2D-STE are volume load-dependent and enhanced by cardiac volume loading [27]. On the other hand, the degree of volume load dependency on LA function indices derived from strain imaging using 2D-STE remains unclear in dogs.

Therefore, the aim of this study is to elucidate the effect of clinically relevant changes of acute volume loading on strain and SR parameters derived using the 2D-STE method in dog models. The results of the present study could describe the degree of volume load dependency on LA myocardial deformation for further therapeutic strategy and prognostic information of the LA.

MATERIALS AND METHODS

Animals

Six laboratory beagles (aged 1–3 years, with body weight of 8.8 to 11.4 kg), which were part of an experimental unit at Hokkaido University, were enrolled in this study. All dogs were healthy and had no abnormalities of cardiac function on the basis of routine physical examination, including blood examination, electrocardiogram (ECG), and standard echocardiography (including M-mode, pulsed-wave Doppler, and color flow Doppler–based imaging). All procedures were reviewed and approved by the laboratory animal experimentation committee of the Graduate School of Veterinary Medicine, Hokkaido University (approval No. 15-0087).

Procedure

The protocol used in this study was the same as in a previous report [27]. An intravenous infusion route was established in each dog on the left and right cephalic veins with a 20-gauge over-the-needle catheter, and a 24-gauge over-the-needle catheter was placed in the left or right dorsal pedal artery to directly monitor arterial blood pressure. Each dog was administered atropine sulfate (Mitsubishi Tanabe Pharma Corp., Osaka, Japan) 0.05 mg/kg, subcutaneously, cefazolin sodium hydrate (Astellas Pharma Inc., Tokyo, Japan) 20 mg/kg intravenously (IV), and heparin sodium (Ajinomoto Pharmaceuticals Co., Ltd., Tokyo, Japan) 100 units/kg IV, and sedated with butorphanol tartate (Meiji Seika Pharma Co., Ltd., Tokyo, Japan) 0.2 mg/kg IV and midazolam hydrochloride (Astellas Pharma Inc., Tokyo, Japan) 0.1 mg/kg IV. Then, anesthesia was induced with administration of propofol (Mylan Inc., Canonsburg, PA, U.S.A.) 6 mg/kg IV. Thereafter, each dog was endotracheally intubated, and anesthesia was maintained with isoflurane (DS Pharma Animal Health Co., Ltd., Osaka, Japan) 1.75 to 2.0% in 100% oxygen. End-tidal partial pressure of carbon dioxide was continuously monitored and maintained between 35 and 45 mmHg with mechanical ventilation, with a tidal volume of 10 to 15 m*l*/kg and a respiratory rate of 10 to 12 breaths/min. Heart rate and arterial pressure measured with arterial catheterization were continuously recorded with a commercial polygraph instrument (Nihon Kohden Co., Ltd., Tokyo, Japan).

A 6F, 12-cm introducer sheath (St. Jude Medical Inc., Minnetonka, MN, U.S.A.) was percutaneously inserted into the right external jugular vein using the Seldinger technique in each dog which was positioned in the position of left lateral recumbency. A 5F, 75-cm Swan-Ganz catheter (Edwards Lifesciences Corp., Irvine, CA, U.S.A.) was advanced into the pulmonary artery with fluoroscopy guidance. The catheter was connected to polygraph equipment for acquisition of hemodynamic data.

Following a stabilization period of about 10 min, baseline recordings of hemodynamic and echocardiographic indices were performed. Thereafter, cardiac preload was increased by IV infusion of warmed lactated Ringer solution (Terumo Corp., Tokyo, Japan) at 150 m*l*/kg/hr for 90 min [27]. This dose was modified from the dose used in previous studies [16, 17].

After the fluid infusion began, hemodynamic and echocardiographic evaluations were performed every 15 min. The hemodynamic data were obtained before echocardiography at each time point assessment. Following the final echocardiographic examination, each dog was administered furosemide (Sanofi K K, Tokyo, Japan) 4 to 6 mg/kg IV and allowed to recovery from anesthesia.

Hemodynamic assessment

All hemodynamic data including heart rate, mean arterial blood pressure, mean pulmonary arterial pressure, pulmonary capillary wedge pressure (PCWP), mean right atrial pressure, and cardiac output were recorded by a polygraph instrument and digitally stored. Mechanical ventilation was briefly stopped during the recordings of hemodynamic indices. The distal and proximal ports of a Swan-Ganz catheter were used to measure pulmonary arterial and right atrial pressures, respectively. The PCWP was determined when the balloon at the end of the Swan-Ganz catheter was inflated to be wedged in a small pulmonary artery. After pressure recordings, cardiac output was determined using the thermodilution method with the injection of a 5 m*l* bolus of cold saline (0.9% NaCl) into the right atrium through the proximal port of a Swan-Ganz catheter. Stroke volume was calculated by dividing cardiac output by heart rate. For pressure measurements, the mean of five consecutive cardiac cycles was calculated, and the average of four measurements was calculated for cardiac output.

Standard echocardiographic methods

Echocardiography was performed by the same experienced investigator (KN) using a Toshiba Artida^{TM} echocardiographic system (Toshiba Medical System Corp., Tochigi, Japan) with a 3- to 7-MHz sector probe transducer array. All echocardiographic indices were recorded when dogs were in an expiratory phase. An ECG trace (lead II) was recorded simultaneously with echocardiographic imaging by the ECG equipment on the ultrasonographic device, in addition to that on the polygraph instrument. The mean of 3 consecutive cardiac cycles was calculated for all echocardiographic indices, including those determined by 2D-STE.

Pulsed-wave Doppler echocardiography was performed to measure the transmitral flow velocity from the left apical four-chamber view. The sample gate for transmitral flow was placed at the tip of the mitral valve leaflets when they were opened [3]. The following indices were measured: peak velocity of the early diastolic wave (E wave), peak velocity of the late diastolic wave (A wave), and the ratio of the peak velocity of the E wave to the peak velocity of the A wave. These indices were not determined when the E and A waves were completely or partially fused.

The aortic Doppler flow profile was obtained with the sample gate positioned immediately below the aortic valve from the left apical five-chamber view. Left ventricular ejection time (ET) was measured as the interval from the onset to the end of the aortic flow. Left ventricular pre-ejection period (PEP) was measured as the interval from the start of the QRS complex to the beginning of aortic flow. The ratio of the PEP to ET was calculated.

Myocardial motion velocities derived from tissue Doppler imaging were recorded with the sample gate placed at the septal mitral annulus from the left apical four-chamber view [3]. The peak velocity of the systolic wave (S′ wave), peak velocity of the early diastolic wave (E′ wave), and peak velocity of the late diastolic wave (A′ wave) were measured, and the ratio of the peak velocity of the E′ wave to the peak velocity of the A′ wave and the ratio of the peak velocity of the E wave to the peak velocity of the E′ wave were calculated. These indices other than the peak velocity of the S′ wave were not determined when the E′ and A′ waves were completely or partially fused.

Additionally, from the tissue Doppler imaging velocities of myocardial motion at the septal mitral annulus, the isovolumic relaxation time (IVRT) and the isovolumic contraction time (IVCT) was measured: the IVRT was correspondence to the interval from the end of the S′ wave to the beginning of the E′ wave, while the IVCT was correspondence to the interval from the end of the A′ wave to the beginning of the S′ wave.

2D-STE of the LA

From the left apical four-chamber view, the image used for strain imaging using 2D-STE of LA was acquired with the frequency, depth, and sector width adjusted for optimization of frame rate (between 151 and 229 frames per rate). The image of three consecutive cardiac cycles was digitally stored at each assessment point for later offline analysis.

The obtained echocardiographic images were analyzed with 2D wall motion-tracking software (Toshiba Medical Systems Corp., Tochigi, Japan) by one investigator (AD) [5, 25]. The LA strain and SR were analyzed by 2D-STE using the QRS complex on the ECG trace as the initiation of the calculation. The LA endocardial surface was manually traced along the clearly visualized internal edge of the LA wall in that frame using the point-and-click method, and the epicardial surface of the LA wall was automatically generated by offline software. After tracking, the software generates an optimal region of interest with the LA myocardial wall thickness divided into six segments with adjustable width to fit the entire LA myocardial wall throughout the cardiac cycle, thus creating the longitudinal strain and SR curve for each atrial segment and a mean curve of all six segments (global strain and SR) for each dog. A cine loop preview was used to confirm an adequate speckle pattern generation following movement of the LA myocardium. All images included in the study were visually inspected for image quality (an adequate image without dropout speckle pattern). The LA strain and SR for each of the three phasic functions were measured from the global curve at three different time points (Fig. 1) [5, 25]: minimum strain (S_{min}) at negative peak during the ventricular end-diastole, maximum strain (S_{max}) at peak during the ventricular systole, and strain before atrial contraction (S_a). The LA strain corresponding reservoir function (εS), that for conduit function (εE), and that for booster pump function (εA) were calculated at the period of ventricular systole, early ventricular diastole, and late ventricular diastole using the following equations, respectively.

$$\varepsilon S=S_{max}-S_{min,}\ \varepsilon E=S_{max}-S_{a,}\ \varepsilon A=S_a-S_{min}$$

Similarly, the SR for reservoir function (SR_S), SR for conduit function (SR_E), and SR for booster pump function (SR_A) were calculated at the time of ventricular systole at positive peak, early ventricular diastole at first negative peak, and late ventricular diastole at second negative peak, respectively, as follows:

$$SR_S=max1,\ SR_E=min1,\ SR_A=min2$$

As well as LA strain and SR curves, the software automatically generated a LA volume curve which was calculated by the monoplane area-length method of LA. LA volumes for each of the three phasic functions were measured: maximal LA volume (V_{max}), the volume at the frame before the opening of the mitral valve starts; preatrial contraction LA volume (V_{preA}), the volume at the frame before the P wave on the ECG; and minimal LA volume (V_{min}), the volume at the frame at the mitral valve closure. The total, passive, and active LA emptying FVCs indicating reservoir, conduit, and booster pump function, respectively, were calculated based on the following formulae:

$$\text{LA-FVC}_{total}=100\times(V_{max}-V_{min})/V_{max,}$$
$$\text{LA-FVC}_{passive}=100\times(V_{max}-V_p)/V_{max,}$$
$$\text{LA-FVC}_{active}=100\times(V_p-V_{min})/V_p$$

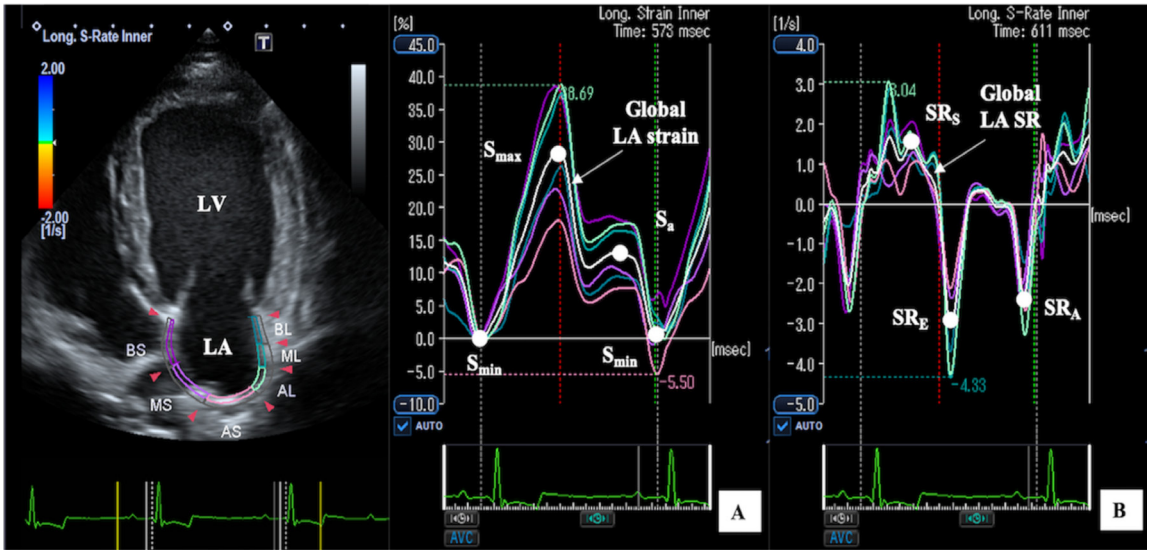

Fig. 1. Two-dimensional speckle tracking echocardiographic images illustrating measurement of strain and strain rate (SR) curves during each phasic function of the left atrium (LA). The LA myocardium was automatically divided into six segments, as shown in the apical four-chamber view. White lines represent the average global strain and SR. From the onset of ventricular systole, the mean LA strain curve presented the first positive peak and decrease to a plateau during diastasis, followed by the second positive peak at the atrial contraction phase, and finally the negative peak after atrial contraction. For the SR profile, the first positive peak during ventricular systole (SR_s) and two negative peaks at early (SR_e) and late (SR_a) ventricular diastole were obtained.

Statistical analysis

Statistical analyses were performed on JMP Pro 12.2.0 software (SAS Institute, Cary, NC, U.S.A.). Normal distribution of the data was confirmed by a Shapiro-Wilk test. A linear mixed model was developed with time (baseline, 15, 30, 45, 60, 75, and 90 min) as a categorical fixed effect and dog identity as a random effect. The *F* test was performed to assess the effect of time on the values of the measured variables. Pairwise comparisons between the baseline and each time point were performed by obtaining the least-squares means and using the Bonferroni correction to account for multiple comparisons. The relationship between PCWP and each of the indices of LA functional strain/SR were investigated using multiple regression analysis. In model 1, the PCWP and dummy coding of the enrolled dogs were included as covariates (linear regression model). In model 2, the quadratic terms of PCWP and dummy coding of the enrolled dogs were entered as covariates (quadratic regression model). For each LA function parameter, model 2 was accepted if the effect of the quadratic term of the PCWP was significant, and a log-likelihood ratio χ^2 test revealed that model 2 had a fit superior to that of model 1. After constructing each model, assumptions of linearity, normality, homoscedasticity, and independence of the residuals were evaluated by inspection of the standardized residual plots and quantile plots.

RESULTS

Change in hemodynamic variables

The changes in hemodynamic variables before (baseline) and at each assessment point after IV infusion of fluid are summarized in Table 1. Mean PCWP and cardiac output were significantly greater than at baseline from 15 to 90 min after acute volume loading began. Heart rate and mean arterial blood pressure were not significantly changed from baseline at 15 to 90 min for all 6 dogs, whereas stroke volume was significantly changed from baseline at 15 to 90 min.

Change in echocardiographic parameters

The changes in echocardiographic parameters before (baseline) and at each assessment point after acute volume loading began are summarized in Table 2. Peak velocities of E, A, E′, and A′ wave were determined without fusion of the E and A wave and the fusion of the E′ wave and A′ wave for all dogs. Acute volume loading induced a significant increase from baseline at 15 to 90 min in peak velocity of the E wave, E′ wave, and at 30 min in the A′ wave. LV ET was significantly increased and the ratio of LV PEP to ET was significantly decreased from baseline at 15 to 90 min. The IVCT and IVRT did not show a significant change after volume infusion. For LA strain and SR variables (Table 3), acute volume loading caused a significantly increased LA strain from baseline, corresponding to reservoir function and conduit function from baseline at 15 to 90 min and at 45 to 90 min in εA (Fig. 2). Acute volume loading caused a significant increase from baseline in all phasic functions of SR at 15 min. The LA volumes and LA-FVCs at each assessment point after acute volume loading are shown in Table 4. The V_{min}, V_{preA}, and V_{max} were obtained from speckle tracking analysis. The V_{preA} was significantly increased from baseline at 60 to 90 min, at 15 to 90 min in V_{max}, and at 75 to 90 min in V_{min}.

Table 1. Least square mean (95% CI) obtained from linear mixed model for hemodynamic data before (baseline) and each times point during acute volume loading in 6 healthy beagles

Variables	Baseline	15 min	30 min	45 min	60 min	75 min	90 min
MBP	55 (48–63)	55 (48–62)	57 (49–64)	58 (51–65)	60 (53–67)	60 (53–67)	59 (52–67)
Heart rate (beats/min)	110 (103–117)	101 (94–108)[a)]	109 (102–116)	110 (103–117)	113 (106–120)	114 (107–121)	109 (102–116)
PAPm (mmHg)	9.5 (7.1–11.9)	12.7 (10.2–15.1)[a)]	15 (12.6–17.4)[a)]	16.3 (13.9–18.8)[a)]	17.3 (14.9–19.8)[a)]	17.8 (15.4–20.3)[a)]	17.5 (15.1–19.9)[a)]
PCWPm (mmHg)	3.3 (1.1–5.6)	8 (5.8–10.2)[a)]	10.3 (8.1–12.6)[a)]	12 (9.8–14.2)[a)]	12.7 (10.4–14.9)[a)]	13.3 (11.1–15.6)[a)]	14 (11.8–16.2)[a)]
RAPm (mmHg)	0.3 (−1.1–1.7)	5.5 (4.1–6.9)[a)]	6.5 (5.1–7.9)[a)]	7.2 (5.8–8.6)[a)]	7.5 (6.1–8.9)[a)]	8.2 (6.8–9.6)[a)]	8.3 (6.9–9.7)[a)]
Cardiac output (*l*/min)	2.1 (1.8–2.4)	2.6 (2.3–2.8)[a)]	2.8 (2.5–3.1)[a)]	2.9 (2.7–3.2)[a)]	3 (2.7–3.3)[a)]	3.1 (2.8–3.4)[a)]	3.1 (2.8–3.4)[a)]
Stroke volume (m*l*)	19 (17–22)	25 (23–28)[a)]	26 (24–28)[a)]	27 (24–29)[a)]	27 (24–29)[a)]	28 (25–30)[a)]	28 (26–31)[a)]

a) Value differs significantly ($P<0.05$) from corresponding baseline value. PAP=Pulmonary arterial blood pressure. RAP=Right atrial blood pressure. PCWP=Pulmonary capillary wedge pressure. MAP=Mean arterial blood pressure as measured via arterial catheterization.

Table 2. Least square mean (95% CI) obtained from linear mixed model for conventional echocardiographic parameters before (baseline) and each times point during acute volume loading in 6 healthy beagles

Variables	Baseline	15 min	30 min	45 min	60 min	75 min	90 min
E wave (m/sec)	0.71 (0.65–0.77)	0.84 (0.78–0.89)[a)]	0.85 (0.79–0.91)[a)]	0.83 (0.77–0.89)	0.91 (0.85–0.97)[a)]	0.91 (0.85–0.97)[a)]	0.85 (0.79–0.91)[a)]
A wave (m/sec)	0.43 (0.33–0.53)	0.48 (0.38–0.58)	0.55 (0.45–0.66)	0.55 (0.45–0.65)	0.53 (0.42–0.63)	0.56 (0.45–0.66)	0.49 (0.38–0.59)
Ratio of E and A	1.72 (1.33–2.10)	1.81 (1.42–2.19)	1.58 (1.19–1.97)	1.66 (1.27–2.05)	1.69 (1.29–2.07)	1.77 (1.39–2.16)	1.86 (1.47–2.25)
PEP (msec)	74 (66–81)	66 (59–74)[a)]	66 (58–73)[a)]	62 (55–70)[a)]	60 (52–67)[a)]	61 (53–68)[a)]	62 (54–69)[a)]
ET (msec)	185 (170–200)	235 (220–250)[a)]	239 (223–254)[a)]	243 (228–258)[a)]	255 (239–270)[a)]	253 (238–269)[a)]	261 (246–276)[a)]
Ratio of PEP and ET	0.40 (0.36–0.44)	0.28 (0.25–0.32)[a)]	0.27 (0.24–0.31)[a)]	0.26 (0.22–0.29)[a)]	0.23 (0.19–0.27)[a)]	0.24 (0.20–0.28)[a)]	0.24 (0.20–0.27)[a)]
E′ wave (cm/sec)	6.47 (4.95–7.98)	9.04 (7.52–10.55)[a)]	9.75 (8.23–11.27)[a)]	9.17 (7.66–10.69)[a)]	9.88 (8.36–11.39)[a)]	9.29 (7.78–10.82)[a)]	8.72 (7.20–10.24)[a)]
A′ wave (cm/sec)	3.54 (2.35–4.73)	4.80 (3.61–5.99)	5.18 (3.99–6.36)[a)]	5.56 (4.37–6.75)[a)]	6.53 (5.34–7.71)[a)]	5.17 (3.98–6.36)[a)]	5.29 (4.09–6.48)[a)]
S′ wave (cm/sec)	5.44 (4.59–6.29)	5.42 (4.57–6.27)	5.56 (4.71–6.41)	5.57 (4.72–6.42)	5.96 (5.11–6.81)	5.75 (4.90–6.59)	5.41 (4.56–6.26)
Ratio of E and E’	11.38 (9.68–13.09)	9.39 (7.68–11.09)	8.98 (7.28–10.69)	9.16 (7.45–10.86)	9.26 (7.55–10.96)	10.17 (8.46–11.88)	9.89 (8.18–11.59)
IVCT	55 (45–64)	49 (40–59)	53 (43–62)	47 (37–57)	46 (36–56)	46 (36–56)	48 (39–58)
IVRT	54 (47–62)	57 (49–64)	59 (51–66)	56 (48–63)	60 (52–67)	59 (52–67)	56 (48–63)

a) Value differs significantly ($P<0.05$) from corresponding baseline value. A wave=Peak velocity of the A wave. A′ wave=Peak velocity of the A′ wave. ET=Left ventricular ejection time. E wave=Peak velocity of the E wave. E′ wave=Peak velocity of E′ wave. IVCT=Isovolumic contraction time. IVRT=Isovolumic relaxation time. PEP=Left ventricular pre-ejection period. S′ wave=Peak velocity of S′ wave.

Table 3. Least square mean (95% CI) obtained from linear mixed model for LA strain and strain rate before (baseline) and each times point during acute volume loading in 6 healthy beagles

Variables	Baseline	15 min	30 min	45 min	60 min	75 min	90 min
εS	19.4 (15.5–23.3)	31.1 (27–35.2)[a)]	32.2 (28.3–36)[a)]	32.5 (28.6–36.4)[a)]	33.9 (30–37.8)[a)]	33.1 (29.3–37)[a)]	30.3 (26.4–34.1)[a)]
εE	13.6 (10.3–16.9)	22.3 (18.9–25.7)[a)]	23.9 (20.7–27.3)[a)]	21.8 (18.5–25.1)[a)]	21.5 (18.2–24.7)[a)]	22.6 (19.3–25.8)[a)]	20.7 (17.4–24)[a)]
εA	5.8 (2.6–8.9)	8.8 (5.5–12)	8.3 (5.1–11.4)	10.4 (7.2–13.5)[a)]	12.1 (8.9–15.3)[a)]	10.4 (7.3–13.6)[a)]	9.7 (6.6–12.9)[a)]
SR_S	1.4 (0.8–2)	2.3 (1.7–2.9)[a)]	2.3 (1.7–2.9)[a)]	2.5 (1.9–3.1)[a)]	3.1 (2.5–3.7)[a)]	2.6 (1.9–3.2)[a)]	2.2 (1.5–2.8)[a)]
SR_E	2.5 (1.9–3.2)	3.5 (2.8–4.1)[a)]	3.3 (2.7–3.9)[a)]	3.2 (2.6–3.8)[a)]	3.4 (2.8–4)[a)]	3.3 (2.7–3.9)[a)]	3.1 (2.5–3.7)[a)]
SR_A	1.3 (0.9–1.7)	1.9 (1.5–2.2)[a)]	1.7 (1.4–2.1)[a)]	1.9 (1.5–2.3)[a)]	1.8 (1.4–2.2)[a)]	1.7 (1.3–2.1)[a)]	1.5 (1–1.9)

a) Value differs significantly ($P<0.05$) from corresponding baseline value. εS/ SR_S, εE/ SR_E, εA/ SR_A represent strain/strain rate during reservoir, conduit and booster pump function, respectively.

A quadratic multiple regression model (model 2) provided to be a better fit model when compared with the linear regression model (model 1) for relationships between PCWP and all phasic functions of LA function indices, including LA strains, SRs, and LA-FVCs (Table 5; Fig. 3).

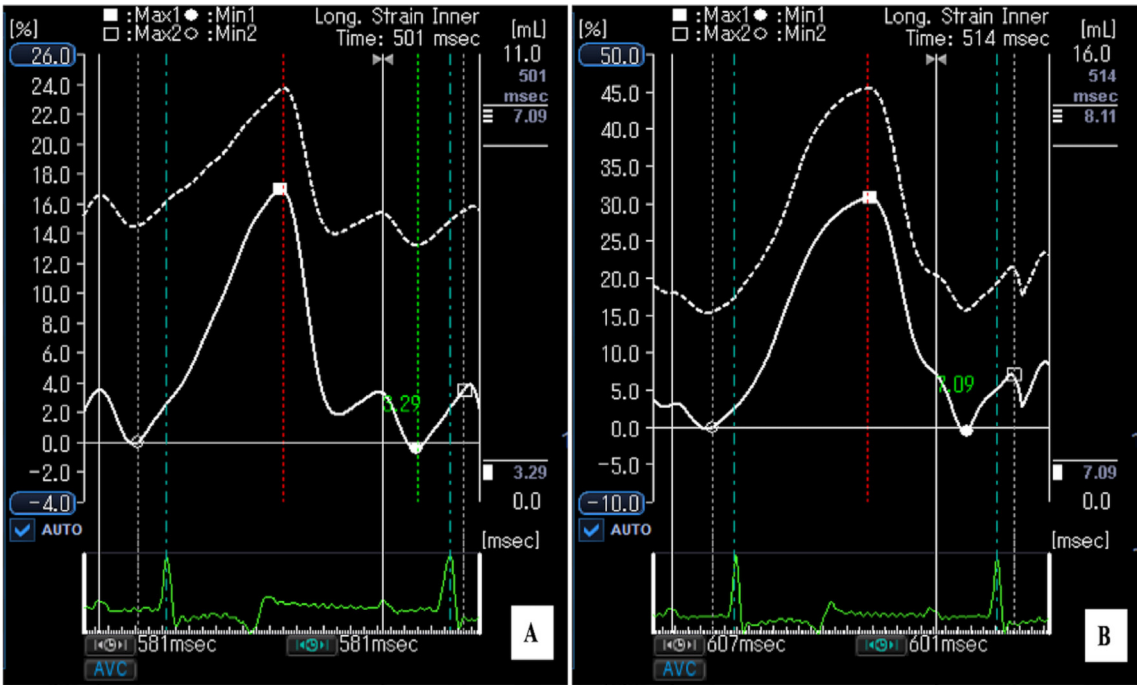

Fig. 2. Representative software generated a strain curve for a single cardiac cycle of a healthy beagle at baseline (A) and at 90 min after cardiac acute volume loading (B).

Table 4. Least square mean (95% CI) obtained from linear mixed model for LA phasic function variables derived from 2D-STE before (baseline) and each times point during acute volume loading in 6 healthy beagles

Variables	Baseline	15 min	30 min	45 min	60 min	75 min	90 min
Vmin	6.12 (4.47–7.77)	6.91 (5.24–8.58)	7.93 (6.29–9.58)	6.66 (5.01–8.30)	7.44 (5.79–9.09)	8.52 (6.87–10.17)[a)]	8.76 (7.11–10.41)[a)]
VpreA	7.31 (4.58–10.04)	8.94 (6.17–11.71)	10.33 (7.60–13.06)	9.33 (6.59–12.06)	10.89 (8.16–13.62)[a)]	11.79 (9.07–14.53)[a)]	11.75 (9.02–14.48)[a)]
Vmax	11.05 (7.03–15.08)	16.63 (12.54–20.71)[a)]	19.19 (15.17–23.22)[a)]	16.59 (12.57–20.62)[a)]	18.83 (14.81–22.86)[a)]	21.19 (17.17–25.22)[a)]	20.51 (16.48–24.53)[a)]
Fractional volume change (%)							
Total	43.6 (38.7–48.4)	58.1 (52.9–63.2)[a)]	58.8 (53.9–63.6)[a)]	59.9 (55–64.8)[a)]	60.1 (55.3–65)[a)]	59.2 (54.4–64.1)[a)]	57.4 (52.5–62.3)[a)]
Passive	32.3 (26.1–38.5)	45.8 (39.4–52.2)[a)]	46.7 (40.5–52.8)[a)]	43.9 (37.7–50.1)[a)]	42.7 (36.5–48.9)[a)]	44.9 (38.7–51.1)[a)]	43.3 (37.1–49.5)[a)]
Active	16.5 (10.2–22.7)	22.9 (16.4–29.4)	22.6 (16.4–28.9)	28.3 (22.1–34.6)[a)]	29.7 (23.5–35.9)[a)]	25.5 (19.3–31.8)[a)]	24.2 (17.9–30.5)[a)]

a) Value differs significantly (P<0.05) from corresponding baseline value. LA-FVC_{total}, LA-$FVC_{passive}$, LA-FVC_{active} represent left atrial fractional volume change during reservoir, conduit and booster pump function, respectively.

Table 5. Maximum likelihood estimates (95% CIs), adjusted coefficients of determination (R^2), and results of log-likelihood ratio χ^2 tests for multiple linear (1) and quadratic (2) regression models of the association between variables of left atrial phasic function and PCWP in 6 healthy Beagles

Variables	Model 1		Model 2			Log-likelihood ratio χ^2 test	
	PCWP	R^2	PCWP	$PCWP^2$	R^2	Accepted	P-value
εS	0.8 (0.4–1.2)	0.55	0.7 (0.5–0.9)	−0.13 (−0.2 to −0.1)	0.79	Q	<0.0001
εE	0.5 (0.3–0.8)	0.50	0.4 (0.2–0.7)	−0.08 (−0.1 to −0.04)	0.68	Q	<0.0001
εA	0.4 (0.2–0.6)	0.64	0.3 (0.1–0.5)	−0.05 (−0.1 to −0.02)	0.72	Q	0.0017
SR_S	0.8 (0.03–0.1)	0.44	0.07 (0.02–0.1)	−0.01 (−0.02 to −0.002)	0.53	Q	0.0067
SR_E	0.05 (0.004–0.1)	0.55	0.03 (−0.01–0.1)	−0.01 (−0.02 to −0.005)	0.68	Q	<0.0001
SR_A	0.03 (−0.003–0.1)	0.42	0.001 (−0.04–0.04)	−0.01 (−0.02 to −0.003)	0.58	Q	0.0067
$LA\text{-}FVC_{Total}$	1.2 (0.7–1.6)	0.53	0.9 (0.6–1.3)	−0.15 (−0.2 to −0.1)	0.77	Q	<0.0001
$LA\text{-}FVC_{Passive}$	0.9 (0.4–1.4)	0.51	0.7 (0.3–1.1)	−0.1 (−0.2 to −0.04)	0.62	Q	0.0017
$LA\text{-}FVC_{Active}$	0.8 (0.4–1.3)	0.59	0.7 (0.3–1.1)	−0.1 (−0.2 to −0.03)	0.67	Q	0.0067

L=Linear regression model (model 1). $PCWP^2$ =Quadratic term of PCWP. Q=Quadratic regression model (model 2).

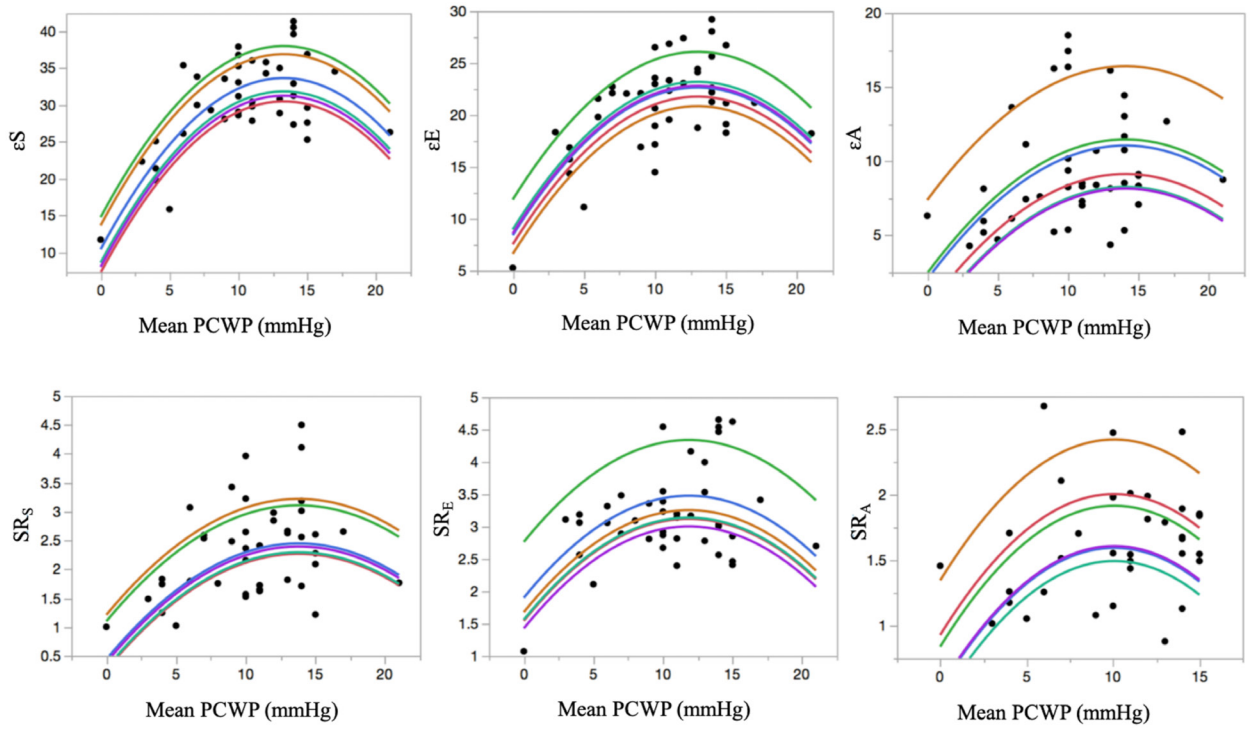

Fig. 3. Relationships between pulmonary capillary wedge pressure (PCWP) in 6 healthy beagles and the following indices of left atrial (LA) phasic function. Quadratic regression lines better fit the relationships between PCWP and LA deformation indices, indicating three phases of LA function.

DISCUSSION

The major finding of our study was that the LA phasic function assessed by strain imaging with 2D-STE was enhanced during experimental cardiac volume overload as the volumetric LA function indices (i.e., LA-FVCs) did. This study was the first to report the relationship between acute volume loading and the three phasic functions of LA obtained via strain imaging with 2D-STE in dogs and to evaluate the response of the strain indices to acute hemodynamic change.

A technical limitation of the volumetric LA function indices including LA-FACs and LA-FVCs is volume load dependency [31]. In heart diseases with volume overload, LA dysfunction evaluated on the basis of these indices can be masked by the enhancing effect of the volume loading on them. In the present study, LA phasic function assessed by LA-FVCs were enhanced with acute volume loading as LA-FACs did in our previous study [27].

Regarding the change in LA phasic function, it is known that there are many significant determinants of cardiovascular factors. The reservoir function is modulated by LA intrinsic relaxation, LA chamber stiffness, and the property of LV contraction [11, 31]. LA conduit function is related to the early diastolic pressure between LA and LV, and relaxation of the LV [31]. The booster pump of LA function is determined by intrinsic LA contractility, LA preload (i.e., LA volume before atrial contraction), and LV end-diastolic filling pressure and compliance [31].

During the early atrial contraction phase, in the same way as for LV, the LA function follows Starling's law, and the booster pump function was enhanced in response to an increasing cardiac preload, as supported by increased volume before atrial contraction (V_{preA}) identified in this study [31].

The increase in volume load enhanced the reservoir function by stimulating the LA booster pump function and LV systolic function as determined by the reduction in the ratio of the LV PEP and ET and by increasing the cardiac output according to the Frank starling mechanism in this study [15, 27, 31, 33].

In addition, the parameter indicating conduit function was higher after infusion of volume. In the study reported here, the peak velocity of the E and the E′ wave was increased with acute volume loading, whereas the ratio of peak velocities of the E to velocity of the E′ wave and the ratio of the velocity of the E to the velocity of the A wave were not changed significantly. The effect of preload on that ratio was suggested as a minimal preload dependency [17]. The enhancement of conduit function was mainly caused by increased LA pressure during the early diastolic period, as suggested by the increase in the indicator of LA pressure (increased peak velocities of E wave) in this study. Mitral valve E velocity is a variable that is not only primarily determined by the filling pressure gradient between LA and LV but also influenced by relaxation [8]. Furthermore, the increase in conduit function might be surpassed by the effect of increased reservoir phase. The LA reservoir and conduit function is correlated with maintaining LV performance, whether the LA is initially filled with blood or volume and consequent relaxation of LV, resulting in increased blood entering the LV. However, the relationship between the LA reservoir and conduit is likely to vary depending on atrial

pressure, volume, and neural control, as described in a previous investigation [29].

In the present study, there were quadratic relationships between PCWP and LA function indices derived from strain imaging with 2D-STE: the LA function indices were initially enhanced and then started to be impaired during cardiac volume overload. This finding is in line with a previous study where the volumetric LA function indices (changes in LA diameter) representing reservoir and booster pump functions were initially enhanced and then impaired in healthy dogs given cardiac volume loading with IV infusion of dextran [15]. During later phases of volume load, results of previous studies suggested that LA afterload, as suggested by an increase in PCWP in this study, could suppress LA booster pump (afterload mismatch of the LA might be induced) and reservoir functions [15, 27]. Indeed, those LA functional parameters during reservoir and booster pump function in this study were not decreased from baseline in the later phase. This observation might imply that the enhancing effect of the volume load of those functions could have been offset by its suppressive effect [27].

There have been conflicting reports between LA function indices determined by strain imaging with 2D-STE in humans. A previous study enrolling infants with patent ductus arteriosus demonstrated that cardiac volume overload secondary to this disease was associated with the impairment of reservoir and booster pump functions evaluated with LA strains and SRs [4]. On the contrary, another previous study including healthy humans showed that the acute decrease in cardiac volume load caused by a tilt maneuver was associated with the impairment of reservoir, conduit, and booster pump functions assessed on the basis of LA strains [10]. The discrepancies between the present study and above-mentioned previous studies might have resulted from the difference in the duration of the change in cardiac volume load, the difference in the degree of the change in cardiac volume load, or the difference in the direction of the change in cardiac volume load.

Several limitations should be noted in this study. First, our study lacked the use of a gold standard for measurement of the mechanical function of the LA. We used a Swan-Ganz catheter and right heart catheterization for measuring hemodynamic variables. LA pressure-volume loop analysis would have strengthened the results. Although the LA pressure-volume loop analysis may be needed to measure LA intrinsic properties [31], the invasive nature of this method and the expertise required to obtain appropriate data limit the application of this approach. In addition, the measurement of LV properties was made only by echocardiographic parameters. Second, we did not measure the LA function indices after examination of diuretic administration. Therefore, it remains unknown whether the LA deformation indices would be decreased after the volume unloading effect. Third, the number of dogs enrolled in study was relatively small, such that we could not determine a significant change in some echocardiographic data. The smaller sample could explain the low power of the statistics. Moreover, we could not clearly determine the indices of conduit and booster pump function in some images, which might possibly be related to the observed increase in the heart rate caused by acute volume loading [18]. Fourth, a possible effect of general anesthesia on cardiac function could not be excluded. As described in a previous study [9], isoflurane alters the active and passive mechanical properties of the LA. This agent can depress LA myocardial contractility, delay relaxation, and also enhance reservoir function [9]. Therefore, the enhancing effect of acute volume loading on LA phasic function in this study might have been affected by the use of isoflurane. Fifth, it is possible that our results could not be extrapolated to dogs with higher PCWP. In the present study, the degree of the elevation of PCWP was relatively mild (mean PCWP of about 15 mmHg). In general, a mean PCWP greater than 15 to 25 mmHg can be associated with left-sided heart failure [7]. Furthermore, this was a clinically normal animal study of the acute volume load effect intervention on the LA strain imaging that we could not exclude the possibility of chronic adaptations in awake clinical dogs. Such chronic adaptations may lead to different response to changes in loading condition.

In conclusion, the LA phasic functions assessed by strain imaging with 2D-STE are affected by changes in acute volume loading condition and correlated with invasive measurement of PCWP in clinically normal dogs. Therefore, the diagnosis on the basis of LA phasic function obtained by strain and SR analysis obtained from 2D-STE should be considered with caution. Strain variables obtained from 2D-STE may serve as a sensitive indicator and provide additional information of the dogs with acute volume loading-stated heart diseases.

ACKNOWLEDGMENTS. The authors did not receive any specific grant for this research from funding agencies in the public, commercial, or not-for-profit sectors. This research was presented as an oral presentation at the 161st meeting of the Japanese Society of Veterinary Science (JSVS) and 2018 ACVR/IVRA Joint Scientific Conference, Omni, Fort Worth, Texas, U.S.A.

REFERENCES

1. Baron Toaldo, M., Romito, G., Guglielmini, C., Diana, A., Pelle, N. G., Contiero, B. and Cipone, M. 2017. Assessment of left atrial deformation and function by 2-Dimensional Speckle tracking echocardiography in healthy dogs and dogs with myxomatous mitral valve disease. *J. Vet. Intern. Med.* **31**: 641–649. [Medline] [CrossRef]
2. Baron Toaldo, M., Romito, G., Guglielmini, C., Diana, A., Pelle, N. G., Contiero, B. and Cipone, M. 2018. Prognostic value of echocardiographic indices of left atrial morphology and function in dogs with myxomatous mitral valve disease. *J. Vet. Intern. Med.* **32**: 914–921. [Medline] [CrossRef]
3. Boon, J. A. 2011. Veterinary Echocardiography, 2nd ed., pp. 153–266 (Boon, J. A. ed), Wiley-Blackwell, Ames.
4. de Waal, K., Phad, N. and Boyle, A. 2018. Left atrium function and deformation in very preterm infants with and without volume load. *Echocardiography* **35**: 1818–1826. [Medline] [CrossRef]
5. Dermlim, A., Nakamura, K., Morita, T., Osuga, T., Nisa, K., Sasaoka, K., Leela-arporn, R., Sasaki, N., Ohta, H. and Takiguchi, M. 2019. The repeatability and left atrial strain analysis obtained via speckle tracking echocardiography in healthy dogs. *J. Vet. Cardiol.* **23**: 69–80. [CrossRef]
6. Dickson, D., Caivano, D., Matos, J. N., Summerfield, N. and Rishniw, M. 2017. Two-dimensional echocardiographic estimates of left atrial function

in healthy dogs and dogs with myxomatous mitral valve disease. *J. Vet. Cardiol.* **19**: 469–479. [Medline] [CrossRef]
7. Drazner, M. H., Prasad, A., Ayers, C., Markham, D. W., Hastings, J., Bhella, P. S., Shibata, S. and Levine, B. D. 2010. The relationship of right- and left-sided filling pressures in patients with heart failure and a preserved ejection fraction. *Circ. Heart Fail.* **3**: 202–206. [Medline] [CrossRef]
8. Garcia, M. J., Ares, M. A., Asher, C., Rodriguez, L., Vandervoort, P. and Thomas, J. D. 1997. An index of early left ventricular filling that combined with pulsed Doppler peak E velocity may estimate capillary wedge pressure. *J. Am. Coll. Cardiol.* **29**: 448–454. [Medline] [CrossRef]
9. Gare, M., Schwabe, D. A., Hettrick, D. A., Kersten, J. R., Warltier, D. C. and Pagel, P. S. 2001. Desflurane, sevoflurane, and isoflurane affect left atrial active and passive mechanical properties and impair left atrial-left ventricular coupling in vivo: analysis using pressure-volume relations. *Anesthesiology* **95**: 689–698. [Medline] [CrossRef]
10. Genovese, D., Singh, A., Volpato, V., Kruse, E., Weinert, L., Yamat, M., Mor-Avi, V., Addetia, K. and Lang, R. M. 2018. Load Dependency of Left Atrial Strain in Normal Subjects. *J. Am. Soc. Echocardiogr.* **31**: 1221–1228. [Medline] [CrossRef]
11. Grant, C., Bunnell, I. L. and Greene, D. G. 1964. The reservoir function of the left atrium during ventricular systole: An angiocardiographic study of atrial stroke volume and work. *Am. J. Med.* **37**: 36–43. [Medline] [CrossRef]
12. Hoit, B. D. 2014. Left atrial size and function: role in prognosis. *J. Am. Coll. Cardiol.* **63**: 493–505. [Medline] [CrossRef]
13. Höllmer, M., Willesen, J. L., Tolver, A. and Koch, J. 2013. Left atrial volume and phasic function in clinically healthy dogs of 12 different breeds. *Vet. J.* **197**: 639–645. [Medline] [CrossRef]
14. Höllmer, M., Willesen, J. L., Tolver, A. and Koch, J. 2016. Comparison of four echocardiographic methods to determine left atrial size in dogs. *J. Vet. Cardiol.* **18**: 137–145. [Medline] [CrossRef]
15. Hondo, T., Okamoto, M., Kawagoe, T., Yamane, T., Karakawa, S., Yamagata, T., Matsuura, H. and Kajiyama, G. 1997. Effects of volume loading on pulmonary venous flow and its relation to left atrial functions. *Jpn. Circ. J.* **61**: 1015–1020. [Medline] [CrossRef]
16. Hori, Y., Ukai, Y., Uechi, M., Hoshi, F. and Higuchi, S. 2008. Relationships between velocities of pulmonary venous flow and plasma concentrations of atrial natriuretic peptide in healthy dogs. *Am. J. Vet. Res.* **69**: 465–470. [Medline] [CrossRef]
17. Hori, Y., Kunihiro, S., Hoshi, F. and Higuchi, S. 2007. Comparison of the myocardial performance index derived by use of pulsed Doppler echocardiography and tissue Doppler imaging in dogs with volume overload. *Am. J. Vet. Res.* **68**: 1177–1182. [Medline] [CrossRef]
18. Horwitz, L. D. and Bishop, V. S. 1972. Effect of acute volume loading on heart rate in the conscious dog. *Circ. Res.* **30**: 316–321. [Medline] [CrossRef]
19. LeBlanc, N., Scollan, K. and Sisson, D. 2016. Quantitative evaluation of left atrial volume and function by one-dimensional, two-dimensional, and three-dimensional echocardiography in a population of normal dogs. *J. Vet. Cardiol.* **18**: 336–349. [Medline] [CrossRef]
20. Li, S. Y., Zhang, L., Zhao, B. W., Yu, C., Xu, L. L., Li, P., Xu, K., Pan, M. and Wang, B. 2014. Two-dimensional tissue tracking: a novel echocardiographic technique to measure left atrial volume: comparison with biplane area length method and real time three-dimensional echocardiography. *Echocardiography* **31**: 716–726. [Medline] [CrossRef]
21. Mitchell, J. H. and Shapiro, W. 1969. Atrial function and the hemodynamic consequences of atrial fibrillation in man. *Am. J. Cardiol.* **23**: 556–567. [Medline] [CrossRef]
22. Mitchell, J. H., Gupta, D. N. and Payne, R. M. 1965. Influence of atrial systole on effective ventricular stroke volume. *Circ. Res.* **17**: 11–18. [Medline] [CrossRef]
23. Mori, M., Kanzaki, H., Amaki, M., Ohara, T., Hasegawa, T., Takahama, H., Hashimura, K., Konno, T., Hayashi, K., Yamagishi, M. and Kitakaze, M. 2011. Impact of reduced left atrial functions on diagnosis of paroxysmal atrial fibrillation: results from analysis of time-left atrial volume curve determined by two-dimensional speckle tracking. *J. Cardiol.* **57**: 89–94. [Medline] [CrossRef]
24. Nagueh, S. F., Smiseth, O. A., Appleton, C. P., Byrd, B. F. 3rd., Dokainish, H., Edvardsen, T., Flachskampf, F. A., Gillebert, T. C., Klein, A. L., Lancellotti, P., Marino, P., Oh, J. K., Alexandru Popescu, B., Waggoner A. D., Houston, Texas; Oslo, Norway; Phoenix, Arizona; Nashville, Tennessee; Hamilton, Ontario, Canada; Uppsala, Sweden; Ghent and Liège, Belgium; Cleveland, Ohio; Novara, Italy; Rochester, Minnesota; Bucharest, Romania; and St. Louis, Missouri. 2016. Recommendations for the Evaluation of Left Ventricular Diastolic Function by Echocardiography: An Update from the American Society of Echocardiography and the European Association of Cardiovascular Imaging. *Eur. Heart J. Cardiovasc. Imaging* **17**: 1321–1360. [Medline] [CrossRef]
25. Nakamura, K., Kawamoto, S., Osuga, T., Morita, T., Sasaki, N., Morishita, K., Ohta, H. and Takiguchi, M. 2017. Left Atrial Strain at Different Stages of Myxomatous Mitral Valve Disease in Dogs. *J. Vet. Intern. Med.* **31**: 316–325. [Medline] [CrossRef]
26. Nakamura, K., Osuga, T., Morishita, K., Suzuki, S., Morita, T., Yokoyama, N., Ohta, H., Yamasaki, M. and Takiguchi, M. 2014. Prognostic value of left atrial function in dogs with chronic mitral valvular heart disease. *J. Vet. Intern. Med.* **28**: 1746–1752. [Medline] [CrossRef]
27. Osuga, T., Nakamura, K., Morita, T., Nisa, K., Yokoyama, N., Sasaki, N., Morishita, K., Ohta, H. and Takiguchi, M. 2016. Effects of experimental cardiac volume loading on left atrial phasic function in healthy dogs. *Am. J. Vet. Res.* **77**: 952–960. [Medline] [CrossRef]
28. Osuga, T., Nakamura, K., Lim, S. Y., Tamura, Y., Kumara, W. R., Murakami, M., Sasaki, N., Morishita, K., Ohta, H., Yamasaki, M. and Takiguchi, M. 2013. Repeatability and reproducibility of measurements obtained via two-dimensional speckle tracking echocardiography of the left atrium and time-left atrial area curve analysis in healthy dogs. *Am. J. Vet. Res.* **74**: 864–869. [Medline] [CrossRef]
29. Payne, R. M., Stone, H. L. and Engelken, E. J. 1971. Atrial function during volume loading. *J. Appl. Physiol.* **31**: 326–331. [Medline] [CrossRef]
30. Roşca, M., Popescu, B. A., Beladan, C. C., Călin, A., Muraru, D., Popa, E. C., Lancellotti, P., Enache, R., Coman, I. M., Jurcuţ, R., Ghionea, M. and Ginghină, C. 2010. Left atrial dysfunction as a correlate of heart failure symptoms in hypertrophic cardiomyopathy. *J. Am. Soc. Echocardiogr.* **23**: 1090–1098. [Medline] [CrossRef]
31. Rosca, M., Lancellotti, P., Popescu, B. A. and Piérard, L. A. 2011. Left atrial function: pathophysiology, echocardiographic assessment, and clinical applications. *Heart* **97**: 1982–1989. [Medline] [CrossRef]
32. To, A. C. Y., Flamm, S. D., Marwick, T. H. and Klein, A. L. 2011. Clinical utility of multimodality LA imaging: assessment of size, function, and structure. *JACC Cardiovasc. Imaging* **4**: 788–798. [Medline] [CrossRef]
33. Wang, Y. P., Takenaka, K., Sakamoto, T., Amano, W., Watanabe, F., Igarashi, T., Suzuki, J., Aoki, T., Sonoda, M., Mashita, M., Tomaru, T., Uchida, Y., Toyo-Oka, T. and Omata, M. 1993. Effects of volume loading, propranolol, and heart rate changes on pump function and systolic time intervals of the left atrium in open-chest dogs. *Acta Cardiol.* **48**: 245–262. [Medline]
34. Wesselowski, S., Borgarelli, M., Bello, N. M. and Abbott, J. 2014. Discrepancies in identification of left atrial enlargement using left atrial volume versus left atrial-to-aortic root ratio in dogs. *J. Vet. Intern. Med.* **28**: 1527–1533. [Medline] [CrossRef]